Immunology and Cell Biology (2010) 88, 172–179

www.nature.com/icb

ORIGINAL ARTICLE

Agent-based simulation of T-cell activation and proliferation within a lymph node

Gib Bogle[1,2] and P Rod Dunbar[1,3]

Recent intravital microscopy experiments have revealed the complex behavior of T cells within lymph nodes. Modeling T-cell responses in lymph nodes now requires integration of cell trafficking and motility with the molecular processes involved in T-cell activation. We describe an agent-based model that allows such integration, in which T cells undertake a random walk through a three-dimensional representation of the lymph node paracortex, integrating signals from dendritic cells (DCs), and proliferating in response. The model accommodates simulation of a large number of T cells packed at realistic densities, and includes dynamic cell trafficking that allows the lymph nodes to swell and shrink as the immune response progresses. The results from the model, including the kinetics of cognate T-cell proliferation and release, and the changes in their avidity profile, are similar to those observed *in vivo*. We therefore propose that this modeling framework is capable of successfully simulating T-cell activation while also accounting for new spatiotemporal knowledge of how T cells and DCs interact. Although some of the parameters used to drive the model are not yet experimentally validated, the model is capable of testing the effects of alternative values for any parameter on the T-cell response. We intend to refine each aspect of the model in collaboration with both theoreticians and experimentalists.
Immunology and Cell Biology (2010) **88,** 172–179; doi:10.1038/icb.2009.78; published online 3 November 2009

Keywords: activation; agent-based; paracortex; proliferation; simulation; T cell

Many adaptive immune responses begin in lymph nodes (LNs), when dendritic cells (DCs) showing identifiable fragments of a pathogen meet up with T cells able to recognize and respond to these antigens. We now know many of the details of how T cells and DCs interact within LNs, but a new level of complexity, only recently appreciated, relates to T-cell motility. In the past few years, advances in microscopy have revealed a wealth of detail about how T cells move within LNs and how they make contact with DCs in both the presence and the absence of their cognate antigen.[1–6] T-cell movement appears to be largely random (best described as a 'random walk'), and T-cell activation results from a series of encounters with DCs bearing antigen, rather than a single long binding event. This complexity means it is no longer sufficient to conceptualize the initiation of T-cell responses in LNs without considering spatial and temporal aspects of cell behavior. The aim of this study was therefore to describe a modeling framework capable of successfully simulating T-cell activation while also accounting for new knowledge of their motility and interactions with DCs, within a three-dimensional (3D) space that simulates the dynamic cell trafficking of the LN.

Most previous models of T-cell activation have taken a 'mean field' approach, using differential equations or probabilistic methods, or a combination of the two[7–11] to solve for the growth of T-cell numbers, with no distinction made between individual cells. These approaches have the virtue of simplicity, requiring little programming and in the case of the first, taking advantage of the well-established mathematics of systems of ordinary differential equations (ODE). However, given the very different paths and encounters that each T cell may undertake within an LN, a more natural approach is agent-based modeling.

An agent-based model (ABM) treats the system under consideration as made up of a collection of discrete entities, or agents. ABM concepts have been widely applied in biology over a wide range of scale,[12] from subcellular processes, in which each 'agent' is a molecule,[13,14] to the level of populations of whole organisms.[15] Each agent is tracked through time as it evolves and engages in interactions with its environment, including other agents, according to specified rules. Spatial effects are readily incorporated, and the rules that govern an agent's behavior can be (and usually are) probabilistic. The internal state of an agent may be described by a combination of discrete and continuous quantities; for the latter each agent can contain its own ODE model, driven by external signals. In addition to discrete agents, the overall environment may also include continuous fields of constituents that agents can both influence and sense. Writing 'cell' for 'agent' and 'cytokine' for 'constituent' in the foregoing makes it easy to see why the ABM approach is well suited to modeling cells, as is well illustrated by its application to simulating epithelial cell behavior in wound healing.[16,17]

[1]Maurice Wilkins Centre, University of Auckland, Auckland, New Zealand; [2]Auckland Bioengineering Institute, University of Auckland, Auckland, New Zealand and [3]School of Biological Sciences, University of Auckland, Auckland, New Zealand
Correspondence: Dr G Bogle, Auckland Bioengineering Institute, University of Auckland, Private Bag 92-019, Auckland 1142, New Zealand.
E-mail: g.bogle@auckland.ac.nz
Received 28 May 2009; revised 24 August 2009; accepted 22 September 2009; published online 3 November 2009

Recent review articles[18–20] describe the value of ABMs in immunology. An ABM of B-cell activation in a germinal center has been taken to an advanced level by the MAMOCELL project.[21,22] A two-dimensional (2D) ABM approach was recently used to compare rates of T-cell activation under conditions where T-cell motility was random or driven by chemotaxis.[23] Another recent T-cell activation model[24] simulated T cells moving on a 3D lattice and investigated the transition in T-cell behavior from rapid scanning of DCs to more sustained contact following antigen recognition.

We recently reported a method[25] for simulating the T-cell motility characteristics derived from intravital microscopy experiments, within a 3D lattice. The ABM model reported here builds on the previous work, to simulate the processes that occur within the paracortex from the first cognate encounters between DC and T cells to the completion of the T-cell response. In presenting the model here, we have chosen simple understandable scenarios to show the model, especially the integration of models of T-cell trafficking, motility and activation. However we emphasize from the outset that this modeling framework is flexible, and can readily accommodate a very diverse set of cells and molecules. For example, to clearly show the modeling approach, we have chosen to show here the interactions of a single type of T cell (representing $CD4^+$ T cells) with a single type of DC (representing DCs migrating into the paracortex from the periphery). Yet the modeling framework imposes no limit on the number of cell subsets, each with its own preprogrammed rules of behavior, and subsequent iterations of the model will include such diversity—from multiple populations of DCs, to different T-cell subsets (for example, $CD4^+$/$CD8^+$/Treg and/or naive/memory) with different functional properties.

Although our model has some points of similarity with the other models mentioned above, we believe it represents the first attempt at a comprehensive representation of T-cell responses at the scale of an LN lobule. In contrast to much modeling in biology, which tends to focus on the details of processes, the intent here is to integrate information over a range of scale, consistent with the aims of the IUPS Physiome Project.[26,27]

RESULTS

Variable behavior of individual T cells

After some initial experimentation to establish baseline parameters, we run simulations with 10^5 T cells in the DCU, along with 518 DCs, for the steady-state situation in the absence of infection. In this case T-cell trafficking is constant and there are no cognate interactions between T cells and DCs. As we have previously reported,[25] the paths of each T cell through the DCU in the model are random, and the speeds and motility coefficients of each cell are consistent with the ranges observed by intravital microscopy (data not shown). This individualistic behavior of each cell is illustrated in Figure 1. Setting a T-cell inflow rate of 4170 per hour achieved a mean transit time through the DCU of 24 h as expected (see Methods); however the individual transit times of 10^5 T cells passing through the DCU were highly variable (Figure 1), as a result of the independent behavior of each T cell. For simplicity, no constraints were placed on a cell's transit time, so some cells transited very quickly between the entry points randomly located in the upper hemisphere of the DCU and the exit points randomly located in the lower hemisphere (Figure 1).

During each individual T cell's transit through the DCU, it encountered the DCs present at random, and bound to any DC for a (random) time consistent with observations of noncognate interactions *in vivo*. Although T cells were briefly prohibited from binding again to a DC they had just left, their random movement meant they often bound DCs more than once. Analysis of the run described above (10^5 T cells, 518 DCs) showed that the average number of distinct DCs contacted by a T cell was 93, with a wide variation in the number of DCs visited by any one T cell (Figure 2). The mean of 93 visits represented around 18% of the available DCs, but in addition an average of 78 repeat contacts occurred between T cells and DCs they had already bound. The rate of T cell–DC encounters per DC is (T-cell inflow rate)×(average number of DCs contacted by a T cell)/(number of DCs), therefore on average each DC scans 749 distinct T cells per hour, and 1377 T cells per hour. For comparison, *in vivo* microscopy yielded scanning rates of 500 for $CD8^+$ and 4630 for $CD4^+$ cells.[1,3]

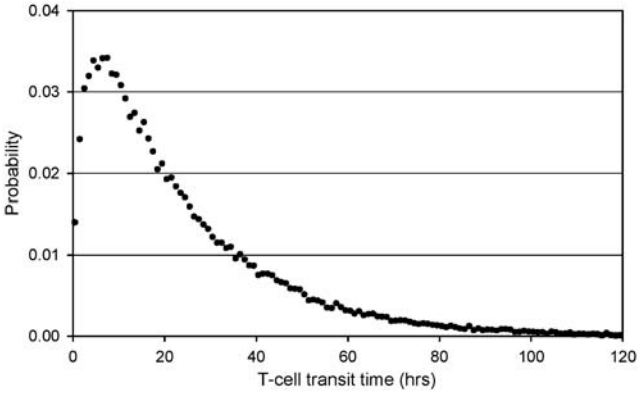

Figure 1 Probability distribution of T-cell transit time, for the steady-state case (no infection) with 10^5 T cells, 518 dendritic cells (DCs) and an average transit time of 24 h. T cells enter at randomly distributed locations in one hemisphere of the blob and leave at random locations in the other hemisphere.

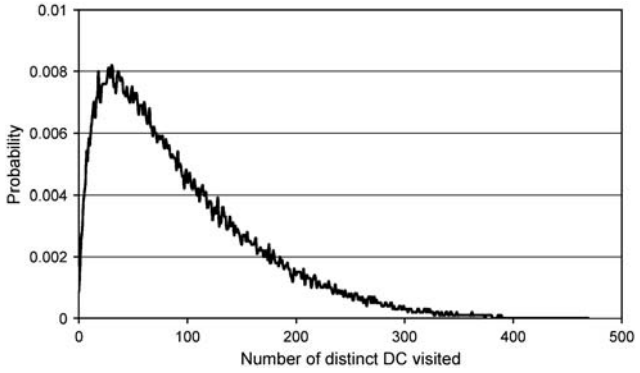

Figure 2 Probability distribution of the number of distinct dendritic cells (DCs) visited by a T cell in its transit through the deep cortical unit (DCU). Steady-state case (no infection), with 10^5 T cells and 518 DCs.

Sensitivity analysis

The model has a large number of parameters, as listed in Supplementary information. Parameter specification is a significant problem,[20] and in the absence of precise measurements of all parameters, some parameters must be estimated to allow the model to run. Model parameters have therefore been set initially at values that, operating together, generate an immune response that looks realistic. Sensitivity studies have then been carried out, by varying a small subset of

parameters, while holding the others fixed. Apart from visual representations of the cells, the main outputs of any simulation run are two proliferation time plots, one showing the total population of activated cells in the paracortex, the other showing the rate of release of activated cells into the circulation. In addition, at each time point the population of activated cells in the blood is described by a 'generation profile', that is, by a histogram showing the numbers of cells in each generation cohort. Finally, as the 'naive' cognate cells can have a range of avidities assigned, and these affect the stimulation each T cell receives from antigen-loaded DCs, changes in the avidity profile of the responding T cells can also be tracked over time.

The first group of sensitivity analyses relate to the size of the T-cell population within the DCU. DCU size clearly varies—in our laboratory's histological observations of serial sections of human LNs, DCU diameters range between 400 and 600 μm at the very least (Angel *et al.*;[28] data not shown). Although not conclusive, these numbers imply DCU T-cell populations of 1 to 4×10^5 (assuming that T cells occupy about 60% of the DCU volume). To explore the influence of T-cell numbers on the size of the response, we stimulated four cases over 10 days, with the initial T-cell population ranging from 0.25 to 2×10^5. In these runs, 10^{-4} of the T cells were designated as cognate and underwent a different program of interaction with antigen-loaded DCs from noncognate T cells. T-cell inflow was adjusted to maintain the population of cells with equivalent residence times across the different T-cell population cases. Table 1 shows the results, based on all the activated cells that exited the LN over the 10 days simulated, whereas the generation profiles of the activated cell populations are compared in Figure 3 (note that the fate of cells after they return to the circulation is not modeled).

These results indicated that the modeled response scales approximately linearly with the initial number of T cells as expected, and the activated T-cell populations for the four cases have very similar generation profiles. The rate of release of activated T cells to the circulation for the four cases, per 1000 cells in the initial population, is plotted against time in Figure 4 (the solid line shows the 10^5 cases). Figure 5 shows how the total T-cell population and the number of cognate cells in the blob vary over the simulated period, for the 10^5 cases. At the peak, the total T-cell population is about seven times the initial value, and the population of cognate T cells is 34 600; there were 10 cognate T cells in the blob initially, and 425 more entered the blob over the 10 days.

We have carried out a large number of simulations to explore the sensitivity of the response to various model parameters. Space permits only a brief summary of these results (see Supplementary information for a more detailed account). (1) Varying the cognate fraction F_C over the range 0.00005–0.0002, we found that the simulated response is roughly proportional to F_C. (2) Varying the TCR stimulation rate constant, K_S, is equivalent to scaling either all TCR avidity levels or all DC antigen density levels. As is shown in Supplementary Figure 3, for values of K_S less than about 0.25 the response is completely suppressed, and although there is a range over which it is roughly proportional to K_S, the response tends to plateau at large values of K_S. The generation profiles of cells returned to the circulation do not vary dramatically when K_S exceeds 0.6, but there is significant variation at lower values (see Supplementary Figure 4). (3) Scaling the number of DCs (both the initial number and the rate of arrival) produces an effect on the response that is almost linearly proportional to the DC count, that is, to the available antigen (Supplementary Figure 5). (4) The total response is affected more by DCs arriving later than by those arriving earlier (DCs being programmed with a finite lifespan and diminishing presentation of antigen over time).

Table 1 Results from 10 day simulations with initial T cell populations ranging from 25 000 to 200 000

Blob radius (sites)	*Initial T cells*	*Initial DCs*	*Maximum T cells*	*Dead T cells*	*Activated T cells*
18.4	25 000	129	186 100	5899	12 673
23.1	50 000	259	371 617	12 512	23 821
29.1	100 000	518	742 669	29 370	50 985
36.7	200 000	1040	1486531	68 426	99 785

Abbreviation: DC, dendritic cell.

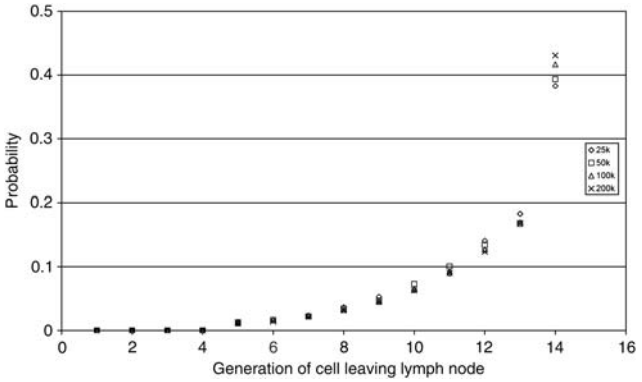

Figure 3 T-cell generation profiles for the activated cells released to the circulation. The profiles are based on all cells that leave the lymph node over the 10 days of the simulation. Results are from simulations in which 1 in 10^4 cells is cognate, and with initial T-cell population $N_0=2.5\times10^4$, 5×10^4, 10^5 and 2×10^5.

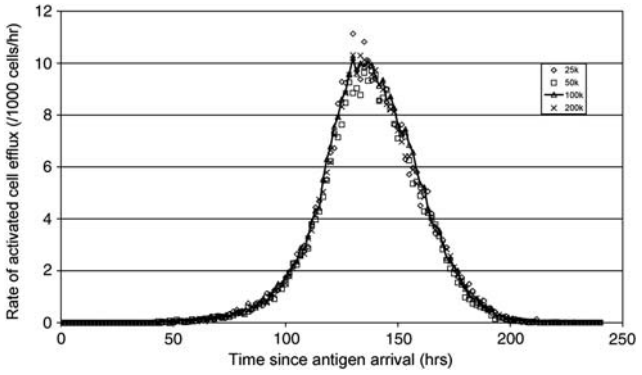

Figure 4 Rate of release of activated T cells to the circulation. The values have been scaled to remove the effect of the number of cells simulated, by plotting the rate of release per 1000 cells in the initial population. The results were derived from simulation runs in which 1 in 10^4 cells is cognate, and with initial T-cell population $N_0=2.5\times10^4$, 5×10^4, 10^5 and 2×10^5.

(5) The model parameter N_B determines the maximum number of cognate T cells that can be in simultaneous contact with a DC, with a value of 15 used in the base case. We obtained a large increase in the response by varying N_B from 1 to 10, but little further change by increasing it up to 20 (see Supplementary Figure 6). Restricting N_B leads to competition for access to antigen and prevents cells from becoming fully activated. (6) The response does not vary much from run to run (with different random number seed values) in cases with 5×10^4 cells or more.

Supplementary Movies 1–6 show cognate T cells and DCs at several stages throughout a simulation run with $N_0=2.5\times10^4$, and Figure 6 shows frames from these movies. In all the preceding response simulations T-cell avidities were drawn from a lognormal distribution, but to explore the influence of avidity an extra case has been simulated with avidity taking a restricted set of discrete values. Supplementary Movie 7 shows the distribution of avidity over the course of the response, for a run in which discrete avidity levels for progenitor cells occur at equal rates. The eight levels, which were chosen such that their logarithms are equally spaced, range from 0.1 to 2.0. Figure 7 shows the corresponding overall distribution of avidity in the final population of antigen-experienced cells, illustrating the selective production of cells with higher avidity.

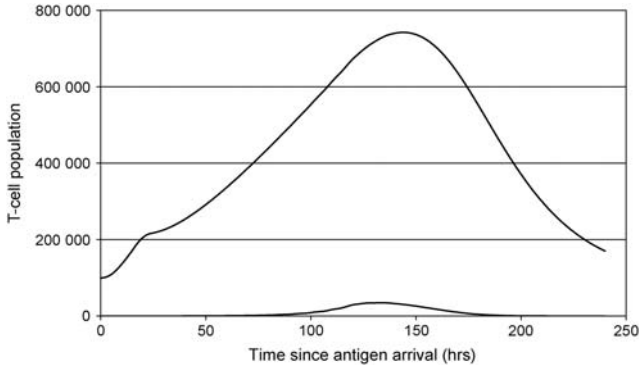

Figure 5 Total number of T cells (top line) and the number of cognate T cells (bottom line), within the simulated deep cortical unit (DCU) for the 10^5 cases, over the 10 days of the simulation. Although the number of cognate (activated) cells increases dramatically over the course of the response, the increase in total cell numbers is largely a result of changes in cell trafficking.

DISCUSSION

The ABM of T-cell activation that we have developed integrates several processes at the scale of a whole DCU, reflecting our conviction that all these processes must be considered simultaneously to generate a realistic model of the immune response. Because the detailed experimental data required to characterize some of these processes are not yet available, we have been forced to make assumptions regarding many of the parameters embedded in the model, but nonetheless the behavior exhibited by the model appears reasonable. In particular the kinetics of both the cognate T-cell responses and the expansion and contraction of the LN DCU are realistic. The capabilities of the model are supported by the sensitivity analysis, where simulations were run with varying parameters, and the characteristics of the T-cell responses compared. These experiments showed the T-cell response generated in the model was sensitive to factors such as the starting frequency of the 'naive' cognate T cells, the rate of influx into the LN of DCs bearing antigen and the timing of the arrival of those DCs.

The lattice geometry offers several advantages. The first of these is speed: because cell motion can be simulated so efficiently it becomes feasible to simulate large numbers of T cells, comparable to the total population of a typical DCU. These T cells are at realistic densities, creating a 'swarm' of cells around the DCs, analogous to that observed *in vivo*. The lattice geometry also permits dynamic adjustment of the size of the modeled region, allowing simulation of expansion and contraction of the LN. Incorporation of 3D fields relating to individual cells is also possible—ideal for simulating cytokine release and uptake on a cell-by-cell basis. As a next step, we are in the process of incorporating IL-2 secretion, uptake and diffusion into the model, and in the future we plan to include other γ-chain cytokines, as well as chemokines.

In the present model the geometry of the DCU is generic, with T cells entering at notional HEVs in one half of the lattice, and leaving

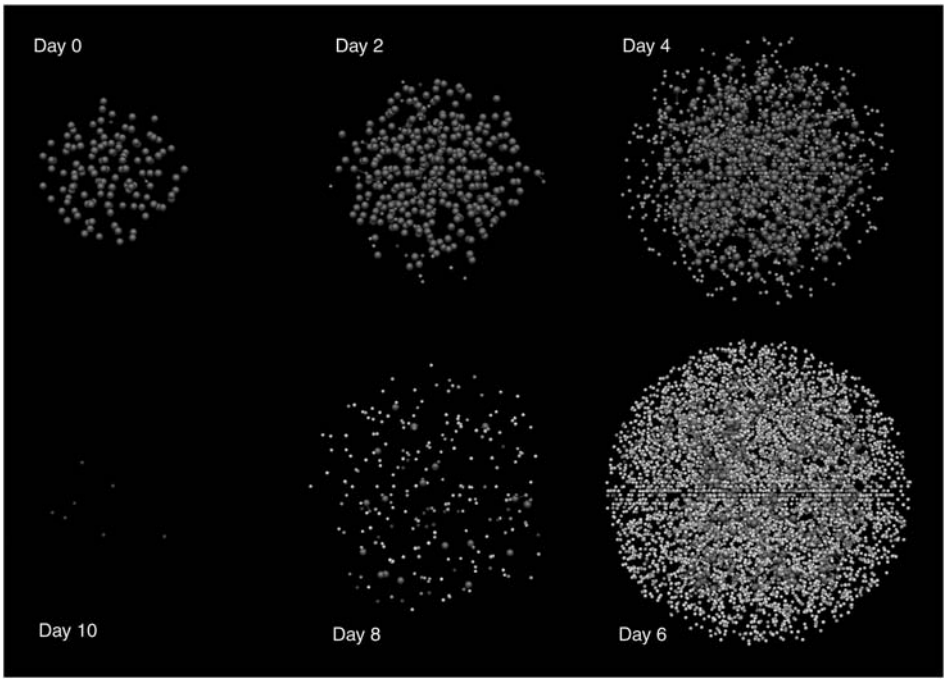

Figure 6 Snapshots at 2-day intervals of the blob for a simulation run with a starting population of 2.5×10^4 T cells (2 cognate T cells) and 129 dendritic cells (DCs). Only DCs and cognate T cells are shown. DCs are shown in green. T cells are deep blue before division, and are colored over a spectrum that shades to yellow as the generation increases to the maximum number of 14. While bound to a DC, T cells are colored red. A full colour version of this figure is available at the *Immunology and Cell Biology* journal online.

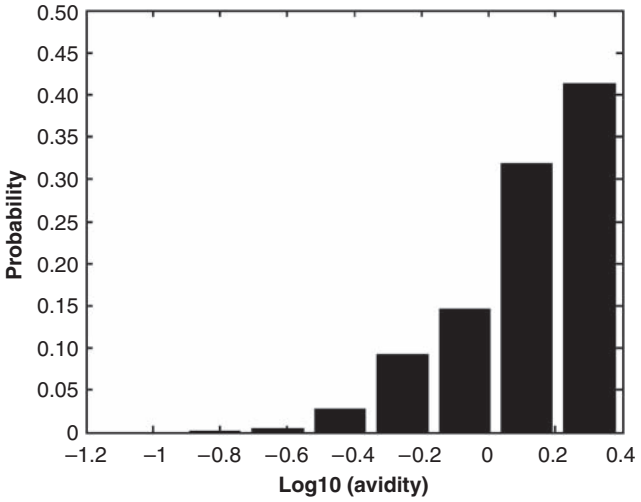

Figure 7 Overall avidity distribution of antigen-experienced cognate T cells at the end of the T-cell response, from a naive population with equal numbers of cells at each discrete avidity level (the levels, which have equally spaced logarithms, are 0.1, 0.153, 0.235, 0.361, 0.554, 0.850, 1.303 and 2.0).

at sinus access points in the other half. Neither the distribution of HEV in LN nor the orientation of exit points into the sinuses are completely understood, but as more details become available of how cells enter and leave the DCU, it will be a simple matter to modify the 'anatomy' of the current model appropriately. The relationship of the entry and exit points also affects the transit times of the T cells. Here there was no restriction on the time between entry and exit, so that some transit times were short (Figure 1). In future it would be simple to impose a lower bound on these times, to prevent T cells that had recently migrated into the DCU from HEVs from migrating across any sinus exit points that they encounter at random,[29] or preferably, to use any physiological rules for such exit control as they become elucidated (for example, CD69 and sphingosine-1-phosphate signaling).

Simulating the DCU at the level shown here can capture aspects of the immune response that are difficult to address in any other way. The original motivation for constructing the model was to enable exploration of spatial effects, specifically the relationship between a T cell's motility behavior and the timing of the response. Intravital microscopy yields a wealth of information within a very restricted 3D region of the LN, whereas histology on sections provides another view, limited by the 2D restriction and the removal of the time element. A 3D simulation model of the whole DCU fills the gap between these two experimental techniques. As better geometrical data become available, they will be readily incorporated into the model, enabling the effects of spatial inhomogeneities of various kinds to be simulated—entry and exit locations, and the distribution of DCs. Looking ahead, we hope to be able to include the influence of cytokines, in which case the model will simulate cytokine concentration fields, which are beyond the reach of current experimental tools.

One of the useful functions of this kind of modeling is to expose gaps in knowledge and understanding. In this case, there are many areas where knowledge is lacking; most notably in the transient modification of the paracortex vascularization, and in the details of the influence of receptor signaling on T-cell activation, especially when T cells are engaging many DCs sequentially. Focusing on the latter immediately shows where future investigation may focus if we are to further our knowledge of how T cells proliferate within the paracortical 'swarm'. In our simulations, cognate T cells underwent their first cell division after encountering several DCs bearing sufficient antigen to trigger signaling through their TCRs (which were assigned different avidities for the antigenic complex on the DC). After that first cell division, the activation level of the T cells decayed, unless they encountered further antigen, and eventually fell to a level where the T cells cease to divide. To refine this aspect of the model, a number of key questions require answers. (1) How does the accumulated level of stimulation provided by TCR-mediated activation (parameter S in our model) decay, and at what rate? (2) What happens to this integrated stimulation level when a cell divides? (3) How does the integrated simulation level influence the number of divisions that a cell undergoes? (4) Do the progeny cells continue to receive and respond to TCR stimulation? If any of these questions can be answered experimentally, the occasionally arbitrary assumptions used in this model will be able to refined considerably.

In some cases it may be difficult to derive parameter values experimentally (for example, the effects of local cytokine concentrations on T-cell activation and proliferation). It is important to note that the model produces outputs that are measurable experimentally—including changes in the numbers of cognate T cells reaching the circulation (measurable using transgenic T cells or peptide–MHC multimers) and their history of cell division (measurable by carboxyfluorescein diacetate succinimidyl ester dilution). This means that parameters that cannot be accurately measured can potentially be 'solved for' to generate a simulation that matches measurable aspects of the T-cell response.

We therefore conclude that the modeling platform we present here is a useful tool for integrating current knowledge about molecular and cellular interactions within LNs, as well as generating new hypotheses to drive new experimental work. It will also be useful in exploring the effects of cellular and molecular mechanisms that we know must exist, but that are not currently accessible to experimentation. We hope that those interested in the initiation of T-cell responses will engage with us to clarify those parameters within the model that can be validated experimentally, and to use the model as an *in silico* laboratory to explore new theories concerning the control of T-cell responses.

METHODS

General description of the model

We aimed to simulate the interactions of T cells and DCs within a single deep cortical unit (DCU) of an LN, during a primary immune response. (The DCU is the region of the paracortex that is densely populated with T cells, for example, see the useful illustration of an idealized LN lobule provided by Willard-Mack.[30]) The model is based on a 3D lattice, as in our previous work,[25] and uses realistic numbers and densities of cells. In the simulations shown here, the model uses a large number of T cells ($\approx 10^5$) to recognition both the number of cells within a DCU, and the low frequency of naive T cells recognizing a particular antigen (in the range of 10^{-6} to 10^{-4}). The cells pack the lattice to the degree that the only space not occupied by T cells and DC is similar to that expected to be occupied by stromal components in real LNs.

Rather than being of fixed size, which would not reflect the true nature of a DCU during an immune response, the modeled DCU is allowed to expand and contract, as T cells migrate in and out, and undergo cell division. T cells migrate into the lattice from points representing the high endothelial venules (HEV), and leave the lattice from randomly assigned points representing points of access to the LN sinuses. The rates of both these migrations are dynamic over time, and changes in migration promote most of the accumulation of T cells in the simulated DCU, just as in a real LN.

The model tracks the interactions of T cells and DCs over a timescale of many days. The T cells undertake a 'random walk' through the DCU, and receive signals through interactions with DCs in their immediate

neighborhood. Parameters for this level of the model derive largely from measurements made using intravital microscopy, including the characteristics of both T-cell motility and T-cell encounters with DCs.[1–6] The internal state of each cell evolves depending on the cell's assigned characteristics, and the signals received from other cells. The integration of signals that determine the activation and proliferation of T cells is based on the ideas of 'signal integration',[31–39] 'progressive differentiation'[40–43] and 'multistage activation'.[4,44]

The model therefore integrates information at a number of levels—T-cell survival and proliferation are based on the internal state of individual T cells; these individual T-cell states are based on their interactions with DCs; these interactions are influenced by the 'random walk' motility of each individual cell, which allows the densely packed cells to behave as a dynamic 'swarm' and the size of the 'swarm' is determined by changes in the rates of T-cell migration in and out of the DCU, as well as the survival and proliferation of individual T cells.

The parameters driving these aspects of the model are described below, and are based where possible on measured values. However, any parameter can also be varied to test its effect on outputs from the model. Outputs include visual representations of the T-cell response over time (see Results), as well as summaries of the behavior of all the cells. Simulations can be run in the absence of cognate interactions between DCs and T cells, for example, to generate results for the transit time of noncognate T cells; or cognate interactions can be initiated, and the T-cell response measured over time. To trigger cognate interactions, a certain number of DCs are programmed to bear an antigen, and a certain number of T cells (usually in the order of 10^{-4}) are designated as cognate for that antigen. Cognate interactions between T cells and DCs differ from noncognate interactions, according to observations from intravital microscopy. The cognate T cells can be assigned a range of avidities for antigen, and the model then tracks both the quantity of the response over time, as the cognate cells proliferate, and the quality of the response, as T cells of different avidity proliferate to different degrees. Simulations begin with a certain number of DCs in the LN, but new DCs also arrive as the simulation progresses. Other functions within the model determine the survival of each DC, its antigen load and the rate at which its antigen presentation decays.

Description of the major parameters driving the model

The parameters of the model are all interlinked, but for convenience they are grouped under subheadings below. Owing to the limited space available, much of the detail has been presented as Supplementary information.

T-cell trafficking. An important parameter to fix at the beginning of our simulations was the residence time (average transit time) within the DCU. Estimates of the residence time of T cells within LNs under baseline (non-reactive) conditions are in the range 12–24 h.[29,45–48] We fixed a residence time of 24 h for all simulations described below. Fixing this parameter rendered the steady-state inflow rate of T cells in each simulation proportional to the T-cell population within the DCU (see Supplementary information); for example, for a T-cell population of 10^5 the inflow rate required was 10^5 cells per 24 h, $\approx$4170 per hour. At steady state, an equivalent number of cells to those arriving at the HEV entry points in the lattice were allowed to exit from the lattice at each time point, as described below.

During an adaptive immune response the rates of inflow and efflux of T cells vary greatly from the steady-state value.[49–51] In reality, the initial expansion in paracortical cellularity is the combined effect of an increase in T-cell inflow, and a transient suppression of efflux in the first $\approx$24 h. Changes in inflow over several days result from transient HEV vascular modification,[52,53] possibly driven by vascular endothelial growth factor (VEGF) secreted by fibroreticular cells in response to inflammation[54–56] (see Supplementary information). The model has therefore linked changes in T-cell inflow to VEGF-driven changes in the volume of the LN vasculature, in response to the amount of antigen arriving into the LN on migrating DCs (as an index of the inflammatory signal from the periphery). Increases in LN vascularity are counteracted by a decay rate term designed to bring vascularization back to the steady-state level when the VEGF concentration declines. T-cell efflux rate is always equivalent to the throughput rate that would maintain the T-cell population steady at its current level, except during the first 24 h of a cognate response, when it is transiently suppressed. This method generates the desired qualitative behavior (as detailed in the Supplementary information), producing expansion of the paracortical population in the early stage of the response, then contraction back to the initial level after the antigen level on the DCs has died away.

T-cell motility and the lattice geometry. The method for simulating T-cell motility is identical to that we previously described[25] with one exception: whereas in the earlier version a random sweep was made in each time step through all lattice sites, in the current version the random sweep is over cells, thus eliminating the possibility of a cell making two jumps in a time step. In this study the motility parameters have been fixed at values that generate a motility coefficient of 64 $\mu m^2\,min^{-1}$ and mean speed of 16 $\mu m\,min^{-1}$, using the model that allows movement in all possible directions (model M26, which allows jumps to all 26 neighbors within a $3\times3\times3$ cube of lattice sites).[25]

Histology reveals the shape of a typical DCU is ellipsoidal,[30] and for programming convenience, the DCU is currently assumed to approximate a sphere, referred to as the 'blob'. A T cell occupies a single site, whereas DCs occupy seven grid sites (a central site and its six neighbors). The quota of sites per DC is rather arbitrary, as data on DC volume are not readily available. Other researchers[57,58] have used volume estimates of 1400 and 2200 μm^3, equivalent to 5.6 and 8.8 sites respectively. Model results are not sensitive to this number, and the value used has the merit of giving symmetry.

In the model presented here, cells enter at randomly chosen sites (representing HEV) in the upper half of the blob, and exit at random sites in the lower half, oriented toward the medulla (the z axis having been chosen arbitrarily as an axis of polarization). Although convenient, the asymmetry in entry and exit locations created a slight gradient in T-cell concentrations, and this was corrected by introducing an adjustment term (a 'drift' factor) into the calculation of jump probabilities, as described in Supplementary information.

When a T cell is added to the blob, either through cell division or by entry through an HEV, the size of the blob is incremented by one (initially vacant) site at the boundary. Similarly, when a cell exits the region or dies a vacant site is removed from the blob at the boundary (seven sites are removed when a DC dies). In this way the number of sites available for cell occupancy always matches exactly the space required by the cells in the blob.

T-cell encounters with DC. A DC soma is surrounded by a conceptual 'sphere of influence' representing the volume swept by the dendrites ($\approx$120 lattice sites as described in Supplementary information). T cells can move freely through this region (except for the seven sites occupied by the DC soma), and have a probability of binding to the DC surface while there. The probability of contact is a simple function of the number of cells that are currently in contact, as a fraction of the maximum number of contacts allowed per DC (currently 100, with a limit of 15 cognate cells), so that as bound T cells detach, new T cells are randomly chosen to take the unoccupied binding sites. The duration of the contact with each DC depends on the antigen specificity and stage of activation of the T cell. Noncognate interactions are short, lasting on average about 3 min, whereas encounters between cognate T cells and DCs can last for hours (see Supplementary information). After detaching there is a short delay during which the cell is not able to contact a DC again. The probabilistic approach to DC binding by T cells, with the current parameter values, ensures that each DC surface remains almost fully occupied by T cells, with the T-cell binding time fitting the distributions observed *in vivo*.

The model begins with a certain number of antigen-bearing DCs randomly positioned in the DCU, and allows for the entry of more antigen-bearing DCs as the response develops. Although these additional DCs could be considered to be arriving from the periphery, the model copes equally well with resident DCs within the DCU taking up antigen transported to the LN by the lymphatics. The rate of 'arrival' of DCs is currently treated in the model as a prespecified function of time, scaled by the initial size of the T-cell population.

T-cell activation and proliferation. When a T cell binds to a DC bearing cognate foreign antigen, an immunological synapse (IS) is formed between the two cells,[59] and T-cell receptors (TCRs) are triggered to transmit a signal to the T-cell interior. The strength of the signal received by the T cell is determined by the total triggering rate of all the TCRs in the IS (in our model the co-stimulation signal is assumed to be always saturating). According to the 'signal integration/progressive differentiation' hypothesis[43] the stimulation signal is summed over time, during the period of binding and also through sequential

DC encounters. Milestones in the activation of a T cell are reached when the integrated stimulation exceeds certain thresholds. The rate of TCR stimulation of a T cell is determined by the avidity of the T cell–DC binding, and by the antigen density on the DC, that is, the number of major histocompatibility complex (MHC) molecules carrying the peptide. In the model the stimulation rate is proportional to the product of the antigen density and the TCR avidity, which are both variable over DCs and cognate T cells, respectively. It is known that a DC's antigen density declines over time, but we do not know yet what determines DC exhaustion. As an interim measure, the current simulations use a half-life of 48 h to represent antigen decay. This value is intended to represent 'a few days', which is the level of precision that is currently available in the literature.

In vivo microscopy experiments have revealed that a cognate T cell passes through several behavioral stages during the 24–36 h after its first encounter with antigen on a DC before its first division.[3,44] The model combines the time schedule of this 'multistage activation' model with TCR signal integration. Rather than completely specify the time spent in the stages of activation, the model optionally makes some stage transitions depend on the attainment of threshold levels of integrated TCR stimulation. Probabilistic effects enter through the chance aspect of DC encounters, and also through the assignment of minimum cell division times as random variates drawn from specified probability distributions. The random division time determines how long after full activation the cell division can proceed, subject to the additional constraint that stimulation must exceed a threshold value. (Specifics of the various probability distributions used in the simulations are given in Supplementary Table 2.)

1 Bousso P, Robey E. Dynamics of CD8+ T cell priming by dendritic cells in intact lymph nodes. *Nat Immunol* 2003; **4**: 579–585.
2 Cahalan MD, Parker I, Wei SH, Miller MJ. Real-time imaging of lymphocytes *in vivo*. *Curr Opin Immunol* 2003; **15**: 372–377.
3 Miller MJ, Hejazi AS, Wei SH, Cahalan MD, Parker I. T cell repertoire scanning is promoted by dynamic dendritic cell behavior and random T cell motility in the lymph node. *Proc Natl Acad Sci USA* 2004; **101**: 998–1003.
4 Miller MJ, Safrina O, Parker I, Cahalan MD. Imaging the single cell dynamics of CD4+ T cell activation by dendritic cells in lymph nodes. *J Exp Med* 2004; **200**: 847–856.
5 Miller MJ, Wei SH, Cahalan MD, Parker I. Autonomous T cell trafficking examined *in vivo* with intravital two-photon microscopy. *Proc Natl Acad Sci USA* 2003; **100**: 2604–2609.
6 Wei SH, Parker I, Miller MJ, Cahalan MD. A stochastic view of lymphocyte motility and trafficking within the lymph node. *Immunol Rev* 2003; **195**: 136–159.
7 Smith JA, Martin L. Do cells cycle? *Proc Natl Acad Sci USA* 1973; **70**: 1263–1267.
8 Gett AV, Hodgkin PD. A cellular calculus for signal integration by T cells. *Nat Immunol* 2000; **1**: 239–244.
9 De Boer RJ, Ganusov VV, Milutinovic D, Hodgkin PD, Perelson AS. Estimating lymphocyte division and death rates from CFSE data. *Bull Math Biol* 2006; **68**: 1011–1031.
10 Ganusov VV, Milutinovic D, De Boer RJ. IL-2 regulates expansion of CD4+ T cell populations by affecting cell death: insights from modeling CFSE data. *J Immunol* 2007; **179**: 950–957.
11 Callard R, Hodgkin P. Modeling T- and B-cell growth and differentiation. *Immunol Rev* 2007; **216**: 119–129.
12 Thorne BC, Bailey AM, Peirce SM. Combining experiments with multi-cell agent-based modeling to study biological tissue patterning. *Brief Bioinform* 2007; **8**: 245–257.
13 Meier-Schellersheim M, Xu X, Angermann B, Kunkel EJ, Jin T, Germain RN. Key role of local regulation in chemosensing revealed by a new molecular interaction-based modeling method. *PLoS Comput Biol* 2006; **2**: e82.
14 Pogson M, Smallwood R, Qwarnstrom E, Holcombe M. Formal agent-based modelling of intracellular chemical interactions. *Biosystems* 2006; **85**: 37–45.
15 Pratt SC, Sumpter DJT, Mallon EB, Franks NR. An agent-based model of collective nest choice by the ant Temnothorax albipennis. *Anim Behav* 2005; **70**: 1023–1036.
16 Walker D, Wood S, Southgate J, Holcombe M, Smallwood R. An integrated agent-mathematical model of the effect of intercellular signalling via the epidermal growth factor receptor on cell proliferation. *J Theor Biol* 2006; **242**: 774–789.
17 Walker DC, Southgate J, Hill G, Holcombe M, Hose DR, Wood SM *et al.* The epitheliome: agent-based modelling of the social behaviour of cells. *Biosystems* 2004; **76**: 89–100.
18 Kirschner DE, Chang ST, Riggs TW, Perry N, Linderman JJ. Toward a multiscale model of antigen presentation in immunity. *Immunol Rev* 2007; **216**: 93–118.
19 Chavali AK, Gianchandani EP, Tung KS, Lawrence MB, Peirce SM, Papin JA. Characterizing emergent properties of immunological systems with multi-cellular rule-based computational modeling. *Trends Immunol* 2008; **29**: 589–599.
20 Bauer AL, Beauchemin CAA, Perelson AS. Agent-based modeling of host-pathogen systems: the successes and challenges. *Inf Sci* 2009; **179**: 1379–1389.
21 Meyer-Hermann ME, Maini PK. Cutting edge: back to 'one-way' germinal centers. *J Immunol* 2005; **174**: 2489–2493.
22 Meyer-Hermann ME, Maini PK. Interpreting two-photon imaging data of lymphocyte motility. *Phys Rev E Stat Nonlin Soft Matter Phys* 2005; **71**: 061912.
23 Riggs T, Walts A, Perry N, Bickle L, Lynch JN, Myers A *et al.* A comparison of random vs chemotaxis-driven contacts of T cells with dendritic cells during repertoire scanning. *J Theor Biol* 2008; **250**: 732–751.
24 Zheng H, Jin B, Henrickson SE, Perelson AS, von Andrian UH, Chakraborty AK. How antigen quantity and quality determine T-cell decisions in lymphoid tissue. *Mol Cell Biol* 2008; **28**: 4040–4051.
25 Bogle G, Dunbar PR. Simulating T-cell motility in the lymph node paracortex with a packed lattice geometry. *Immunol Cell Biol* 2008; **86**: 676–687.
26 Crampin EJ, Halstead M, Hunter P, Nielsen P, Noble D, Smith N *et al.* Computational physiology and the Physiome Project. *Exp Physiol* 2004; **89**: 1–26.
27 Hunter PJ. The IUPS Physiome Project: a framework for computational physiology. *Prog Biophys Mol Biol* 2004; **85**: 551–569.
28 Angel CE, Chen CJ, Horlacher OC, Winkler S, John T, Browning J *et al.* Distinctive localization of antigen-presenting cells in human lymph nodes. *Blood* 2009; **113**: 1257–1267.
29 Cyster JG. Chemokines, sphingosine-1-phosphate, and cell migration in secondary lymphoid organs. *Annu Rev Immunol* 2005; **23**: 127–159.
30 Willard-Mack CL. Normal structure, function, and histology of lymph nodes. *Toxicol Pathol* 2006; **34**: 409–424.
31 Germain RN, Stefanova I. The dynamics of T cell receptor signaling: complex orchestration and the key roles of tempo and cooperation. *Annu Rev Immunol* 1999; **17**: 467–522.
32 Gunzer M, Schafer A, Borgmann S, Grabbe S, Zänker KS, Bröcker EB *et al.* Antigen presentation in extracellular matrix: interactions of T cells with dendritic cells are dynamic, short lived, and sequential. *Immunity* 2000; **13**: 323–332.
33 Friedl P, Gunzer M. Interaction of T cells with APCs: the serial encounter model. *Trends Immunol* 2001; **22**: 187–191.
34 Rachmilewitz J, Lanzavecchia A. A temporal and spatial summation model for T-cell activation: signal integration and antigen decoding. *Trends Immunol* 2002; **23**: 592–595.
35 Faroudi M, Zaru R, Paulet P, Muller S, Valitutti S. Cutting edge: T lymphocyte activation by repeated immunological synapse formation and intermittent signaling. *J Immunol* 2003; **171**: 1128–1132.
36 Celli S, Garcia Z, Bousso P. CD4 T cells integrate signals delivered during successive DC encounters *in vivo*. *J Exp Med* 2005; **202**: 1271–1278.
37 Garcia Z, Pradelli E, Celli S, Beuneu H, Simon A, Bousso P. Competition for antigen determines the stability of T cell-dendritic cell interactions during clonal expansion. *Proc Natl Acad Sci USA* 2007; **104**: 4553–4558.
38 Khanna KM, McNamara JT, Lefrancois L. *In situ* imaging of the endogenous CD8 T cell response to infection. *Science* 2007; **318**: 116–120.
39 Iezzi G, Karjalainen K, Lanzavecchia A. The duration of antigenic stimulation determines the fate of naive and effector T cells. *Immunity* 1998; **8**: 89–95.
40 Langenkamp A, Casorati G, Garavaglia C, Dellabona P, Lanzavecchia A, Sallusto F. T cell priming by dendritic cells: thresholds for proliferation, differentiation and death and intraclonal functional diversification. *Eur J Immunol* 2002; **32**: 2046–2054.
41 Lanzavecchia A, Sallusto F. Dynamics of T lymphocyte responses: intermediates, effectors, and memory cells. *Science* 2000; **290**: 92–97.
42 Lanzavecchia A, Sallusto F. Regulation of T cell immunity by dendritic cells. *Cell* 2001; **106**: 263–266.
43 Lanzavecchia A, Sallusto F. Progressive differentiation and selection of the fittest in the immune response. *Nat Rev Immunol* 2002; **2**: 982–987.
44 Mempel TR, Henrickson SE, Von Andrian UH. T-cell priming by dendritic cells in lymph nodes occurs in three distinct phases. *Nature* 2004; **427**: 154–159.
45 Henrickson SE, von Andrian UH. Single-cell dynamics of T-cell priming. *Curr Opin Immunol* 2007; **19**: 249–258.
46 Lo CG, Xu Y, Proia RL, Cyster JG. Cyclical modulation of sphingosine-1-phosphate receptor 1 surface expression during lymphocyte recirculation and relationship to lymphoid organ transit. *J Exp Med* 2005; **201**: 291–301.
47 Smith ME, Ford WL. The recirculating lymphocyte pool of the rat: a systematic description of the migratory behaviour of recirculating lymphocytes. *Immunology* 1983; **49**: 83–94.
48 Westermann J, Puskas Z, Pabst R. Blood transit and recirculation kinetics of lymphocyte subsets in normal rats. *Scand J Immunol* 1988; **28**: 203–210.
49 Cahill RN, Frost H, Trnka Z. The effects of antigen on the migration of recirculating lymphocytes through single lymph nodes. *J Exp Med* 1976; **143**: 870–888.
50 Catron DM, Itano AA, Pape KA, Mueller DL, Jenkins MK. Visualizing the first 50 h of the primary immune response to a soluble antigen. *Immunity* 2004; **21**: 341–347.
51 Hay JB, Hobbs BB. The flow of blood to lymph nodes and its relation to lymphocyte traffic and the immune response. *J Exp Med* 1977; **145**: 31–44.
52 Soderberg KA, Payne GW, Sato A, Medzhitov R, Segal SS, Iwasaki A. Innate control of adaptive immunity via remodeling of lymph node feed arteriole. *Proc Natl Acad Sci USA* 2005; **102**: 16315–16320.

53 Steeber DA, Erickson CM, Hodde KC, Albrecht RM. Vascular changes in popliteal lymph nodes due to antigen challenge in normal and lethally irradiated mice. *Scanning Microsc* 1987; **1**: 831–839.
54 Chyou S, Ekland EH, Carpenter AC, Tzeng TC, Tian S, Michaud M *et al.* Fibroblast-type reticular stromal cells regulate the lymph node vasculature. *J Immunol* 2008; **181**: 3887–3896.
55 Jain RK. Molecular regulation of vessel maturation. *Nat Med* 2003; **9**: 685–693.
56 Webster B, Ekland EH, Agle LM, Chyou S, Ruggieri R, Lu TT. Regulation of lymph node vascular growth by dendritic cells. *J Exp Med* 2006; **203**: 1903–1913.
57 Beltman JB, Maree AF, de Boer RJ. Spatial modelling of brief and long interactions between T cells and dendritic cells. *Immunol Cell Biol* 2007; **85**: 306–314.
58 Beltman JB, Maree AF, Lynch JN, Miller MJ, de Boer RJ. Lymph node topology dictates T cell migration behavior. *J Exp Med* 2007; **204**: 771–780.
59 Figge MT, Meyer-Hermann M. Geometrically repatterned immunological synapses uncover formation mechanisms. *PLoS Comput Biol* 2006; **2**: e171.

Supplementary Information accompanies the paper on Immunology and Cell Biology website (http://www.nature.com/icb)